Journal of Power Sources 196 (2011) 2037–2045

Contents lists available at ScienceDirect

Journal of Power Sources

journal homepage: www.elsevier.com/locate/jpowsour

Interface reactivity study between $La_{0.6}Sr_{0.4}Co_{0.2}Fe_{0.8}O_{3-\delta}$ (LSCF) cathode material and metallic interconnect for fuel cell

M.R. Ardigò*, A. Perron, L. Combemale, O. Heintz, G. Caboche, S. Chevalier

Département Interface et Réactivité dans les Matériaux, Laboratoire Interdisciplinaire Carnot de Bourgogne (ICB), UMR 5209 CNRS – Université de Bourgogne, 9 Av. Alain Savary, BP 47870, 21078 Dijon Cedex, France

ARTICLE INFO

Article history:
Received 27 July 2010
Received in revised form
17 September 2010
Accepted 21 September 2010
Available online 1 October 2010

Keywords:
SOFC
Electrode reactivity
Cobaltite
Mixed conductor
Cathode
Interconnect

ABSTRACT

Interface reactivity between $La_{0.6}Sr_{0.4}Co_{0.2}Fe_{0.8}O_{3-\delta}$ (LSCF) cathode material and metallic interconnect (Crofer22APU) was investigated in laboratory air at 700 °C. Due to the interconnect geometry, two interfaces have been analysed: (i) interconnect rib/cathode interface (physically in contact); (ii) the interface under the channel of interconnect. In both cases, formation of a parasite phase was observed after various ageing treatments (20 h, 100 h and 200 h). However, the growth of the determined $SrCrO_4$ parasite phase depends on interface type and on ageing time. Two different mechanisms have been established in function of interface type: (i) $SrCrO_4$ phase was formed after solid state diffusion of Cr from metallic interconnect to the cathode; (ii) gas phase reaction induced formation of $SrCrO_4$ under the channel of interconnect. Finally, the influence of a chemical etching on cathode/interconnect reactivity was evaluated.

1. Introduction

Solid oxide fuel cells (SOFCs) are one of the modern, alternative energy sources that are receiving a lot of attention. Indeed, SOFCs are an environmentally friendly and most efficient power generation technology with low greenhouse gas emission. These systems convert directly the chemical energy of fuels into electricity without combustion and mechanical process [1]. Moreover, they have attracted significant attention due to their high efficiency, fuel flexibility and environmental advantages [2]. Recent researches permitted to decrease the operating temperature of SOFCs from 800–1000 °C to 600–800 °C. This reduction in operating temperature enables the use of metallic materials with higher electronic conductivity, better mechanical property, higher thermal conductivity, better workability and lower cost to replace ceramic materials as the interconnect [3–5]. Note that interconnect is one of the key components in planar SOFCs to connect electrically individual cells in series to make stack and generate high power output with high voltage [6].

In one hand, interconnects must exhibit excellent electrical conductivity and excellent oxidation resistance in air and in H_2/H_2O atmosphere. It should display exceptionally low permeability for oxygen and hydrogen to minimize the direct combination of oxidant and fuel during cell operation; it should possess fairly good thermal conductivity ($5\,W\,m^{-1}\,K^{-1}$ is considered to be the low limit) and its thermal expansion coefficient (TEC) should be comparable to those of electrodes. Moreover, interconnects must exhibit chemical and physical compatibility and stability with adjoining electrodes. Chromia forming alloys are very good candidates as metallic interconnects because of their good matching in thermal expansion with other components of the SOFC [7]. Cofer22APU material, which is one of them, has been developed especially as SOFCs interconnects [8–10] for an operating temperature above 800 °C.

On the other hand, reduction of the electrolyte thickness, development of new electrode and electrolyte materials, like $(La,Sr)(Co,Fe)O_{3-\delta}$ (LSCF), allowed to decrease operating temperature of SOFCs to 600–800 °C. Lanthanum cobalt ferrite-based perovskites, $(La,Sr)(Co,Fe)O_{3-\delta}$, have been widely investigated as possible cathodes for intermediate-temperature SOFCs (ITSOFCs) because they have high ionic and electronic conductivity, good catalytic activity and oxygen permeability [11–15]. This work is included in the IDEAL Cell (Innovative Dual mEmbrAne fueL Cell) project (Seven Framework Programme: 2008–2012). This innovative fuel cell, which is composed of anodic part of protonic conducting fuel cell and cathodic part of SOFC, is working at around 600–700 °C [16]. In IDEAL Cell conditions, the cathode part is $La_{0.60}Sr_{0.40}Co_{0.20}Fe_{0.80}O_{3-\delta}$ (LSCF); this composition leads

* Corresponding author. Tel.: +33 0380396158; fax: +33 0380396132.
E-mail address: maria-rosa.ardigo@u-bourgogne.fr (M.R. Ardigò).

0378-7753/$ – see front matter © 2010 Elsevier B.V. All rights reserved.
doi:10.1016/j.jpowsour.2010.09.063

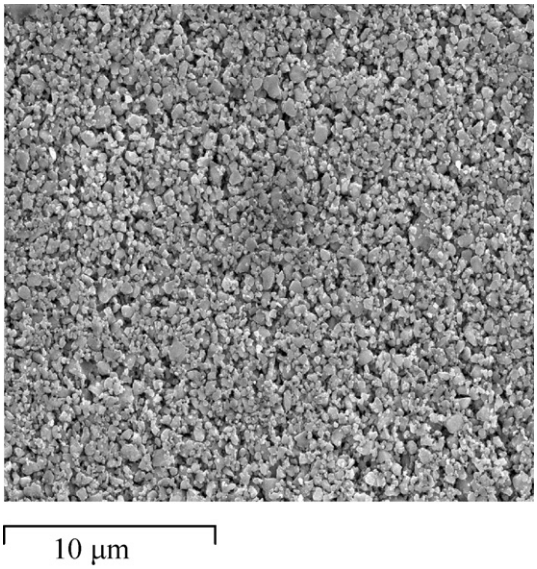

Fig. 1. Cathode surface after sintering at 900 °C for 5 h under laboratory air.

to the best compromise between a high electronic conductivity and a good thermo-mechanical compatibility with the electrolyte material ($Y_{0.15}Ce_{0.85}O_{2-\delta}$) involved in the IDEAL Cell cathodic part [17,18].

So, it appears necessary to investigate the reactivity between cathode material (LSCF) and interconnect (Crofer22APU) at 700 °C. Previous studies have demonstrated that a protective chromia scale grows on the surface at high temperature and confers a good corrosion resistance [4,19]. But, chromium gaseous phases, such as CrO_3 or $CrO_2(OH)_2$, vaporized from the chromia-forming alloy, can have a poisoning effect on electrodes [20] and leads to a rapid deterioration of the performance of SOFC [21–23]. Crofer22APU was developed to form a stable oxide scale such $(Mn,Cr)_3O_4$ spinel phase on top layer. The formation of this spinel top layer leads to a significant reduction in Cr vaporization. Indeed, the volatility of Cr from spinel is lower than from chromia [24,25]. We have already observed the formation of $SrCrO_4$ at the LSCF/Crofer22APU interface [18]. $SrCrO_4$ is non conductive and its formation leads to lowering in cathode conductivity and in cathode porosity [23,26]. Moreover, in lanthanum strontium cobaltites, a decrease in the Sr component – due to the formation of $SrCrO_4$ – leads to a modification of the thermal expansion coefficient [17,26]. $SrCrO_4$ formation is thermodynamically favored and kinetically fast. So this parasite phase will be harmful for the long term stability of the fuel cell [26].

In this study, formation of $SrCrO_4$ parasite phase at the cathode (LSCF)/interconnect (Crofer22APU) interface will be highlighted in function of ageing time and interface type (two different mechanisms will be suggested). Previous experiments showed that a pre-oxidation treatment of interconnects was not effective to protect Cr poisoning of the LSCF cathode [27]. In real SOFCs working conditions, electrical contact layers (usually formed by cathode elements) are often applied between the interconnects and electrodes during construction of a SOFC stack, in order to reduce electrode/interconnect interfacial resistances [28,29]. One method is to apply a cathode ink layer on the interconnect surface. If the interconnect surface is smooth it is not possible to have a good adhesion. In order to obtain a rough surface, a chemical etching has been performed on interconnect by using an acid bath. The influence of a chemical etching on cathode/interconnect reactivity was also evaluated.

2. Materials and methods

2.1. Samples preparation

Cathode $La_{0.6}Sr_{0.4}Co_{0.2}Fe_{0.8}O_{3-\delta}$ (LSCF) powder was provided by Marion Technologies. The synthesis process and the properties of these nanometric powders have been described in a previous study [18]. Cathode powder was cold pressed (8 min under 75 MPa) into pellets of 10 mm diameter. Then, pellets were sintered 5 h at 900 °C under laboratory air (heating and cooling ramp equal to 100 °C h^{-1}) in order to obtain a relative density around 50%. Morphology of cathode pellet after sintering is showed in Fig. 1.

Concerning interconnect material, the Crofer22APU ferritic stainless steel (Cr = 22 wt.%, C = 0.01 wt.%, Mn = 0.5 wt.%, Ti = 0.08 wt.%, La = 0.06 wt.% and Fe balance) was provided by ThyssenKrupp VDM. Interconnect samples were cut into coupons (10 mm × 10 mm × 1 mm), polished from 240 to 1200-grit silicon carbide and finally cleaned with ethanol. As shown in Fig. 2(a), channels were machined on one side of these coupons to simulate the classical geometry of interconnectors.

2.2. Oxidation tests under air at 700 °C

In order to study reactivity between cathode and metallic interconnect in SOFCs, sandwich geometries composed of cathode pellets in contact with interconnects material (Fig. 2(a)) were aged for 20, 100 and 200 h at 700 °C in laboratory air. To study atmosphere moisture influence, a sample in contact with an interconnect was aged in dry air for 100 h at 700 °C.

After thermal treatments, two different areas were observed at the cathode/interconnect interface (Fig. 2(b and c)). The first one corresponds to the cathode/interconnect rib interface and the secondly to the cathode/interconnect channel interface.

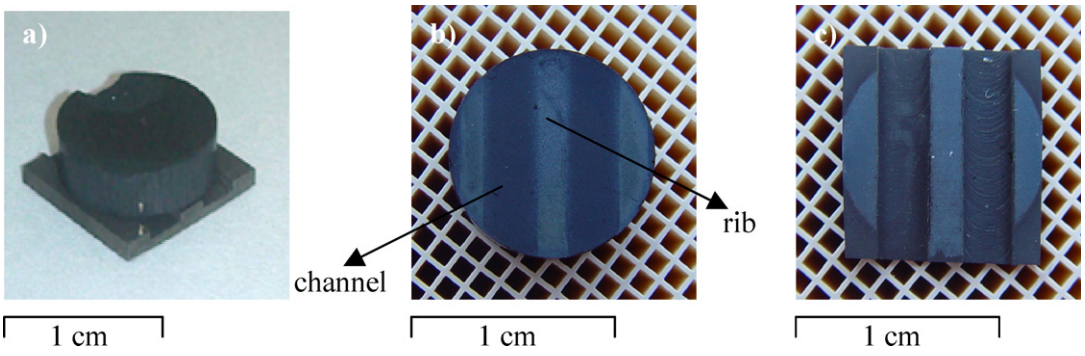

Fig. 2. (a) Cathode on interconnect before ageing test, (b) cathode pellet surface after ageing at 700 °C and (c) interconnect surface after ageing at 700 °C in laboratory air.

Table 1
Acid bath composition.

H_2SO_4 (wt.%)	$Na_2S_2O_3{\cdot}5H_2O$ (g L^{-1})	C_3H_4O (mol L^{-1})	T (°C)	t (min)
5	1.25	0.06	60	25

Table 2
Surface excess before and after sintering at 900 °C for 5 h compared to theoretical composition of a LSCF cathode pellet.

	Element				
	La	Sr	Co	Fe	O
Theoretical at.% composition for $La_{0.6}Sr_{0.4}Co_{0.2}Fe_{0.8}O_{3\pm\delta}$	12	8	4	16	60
% gap between real and theoretical composition	−2	−2	+1	−2	+5
Surface excess after sintering referred to real at.% composition	−3	+3	−4	−8	+12

In order to obtain a rough interconnect surface, in the case that a contact ink layer has to be applied on, a chemical etching was performed on interconnect by using an acid bath. "Conversion bath" used for chemical etching is a solution formed by sulphuric acid, sodium thiosulfate (corrosion activator) and propargylic alcohol (corrosion inhibitor). Different conditions (time and temperature) and concentrations were tested in a previous work [30]. The composition of the bath is given in Table 1. Conditions used are the best for steel grade studied. After chemical etching, stainless steel samples were washed with distilled water and dried at 100 °C for 1 h. Finally, a heat-treatment (450 °C for 2 h) was applied to generate a new phase at the surface of the interconnect. Three different etching times were performed: 25 min, 1 h and 2 h. After the chemical treatment, interconnects were aged on LSCF pellets for 20, 100 and 200 h in laboratory air.

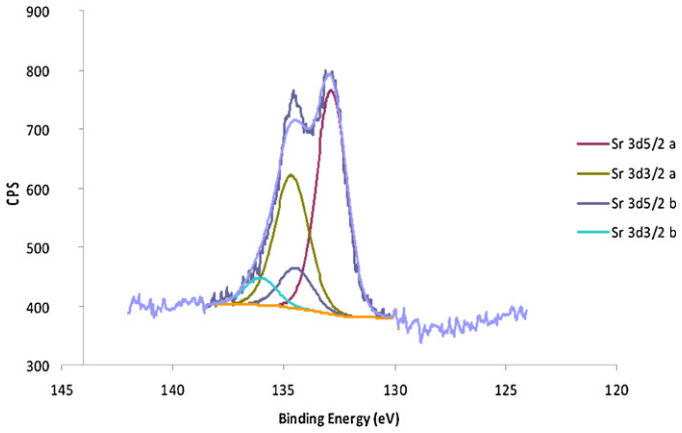

Fig. 3. XPS Sr $3d_{3/2}$–$d_{5/2}$ spectrum of LSCF cathode pellet after sintering for 5 h at 900 °C.

Cathodes and interconnects surfaces were analyzed successively by scanning electron microscopy (SEM – JEOL JSM 6400F) coupled with energy dispersive X-ray analysis (EDX – Oxford Instrument INCA ENERGY microprobe analyzer with pure Co used as standard material), X-ray diffraction (XRD – INEL CPS 120 diffractometer with CuKα radiation source for phase identification) and X-ray photoemission spectroscopy (XPS – PHI 5000 Versa Probe). Moreover interconnect surface was characterized by secondary ion mass spectroscopy (SIMS-CAMECA-RIBER MIQ 256).

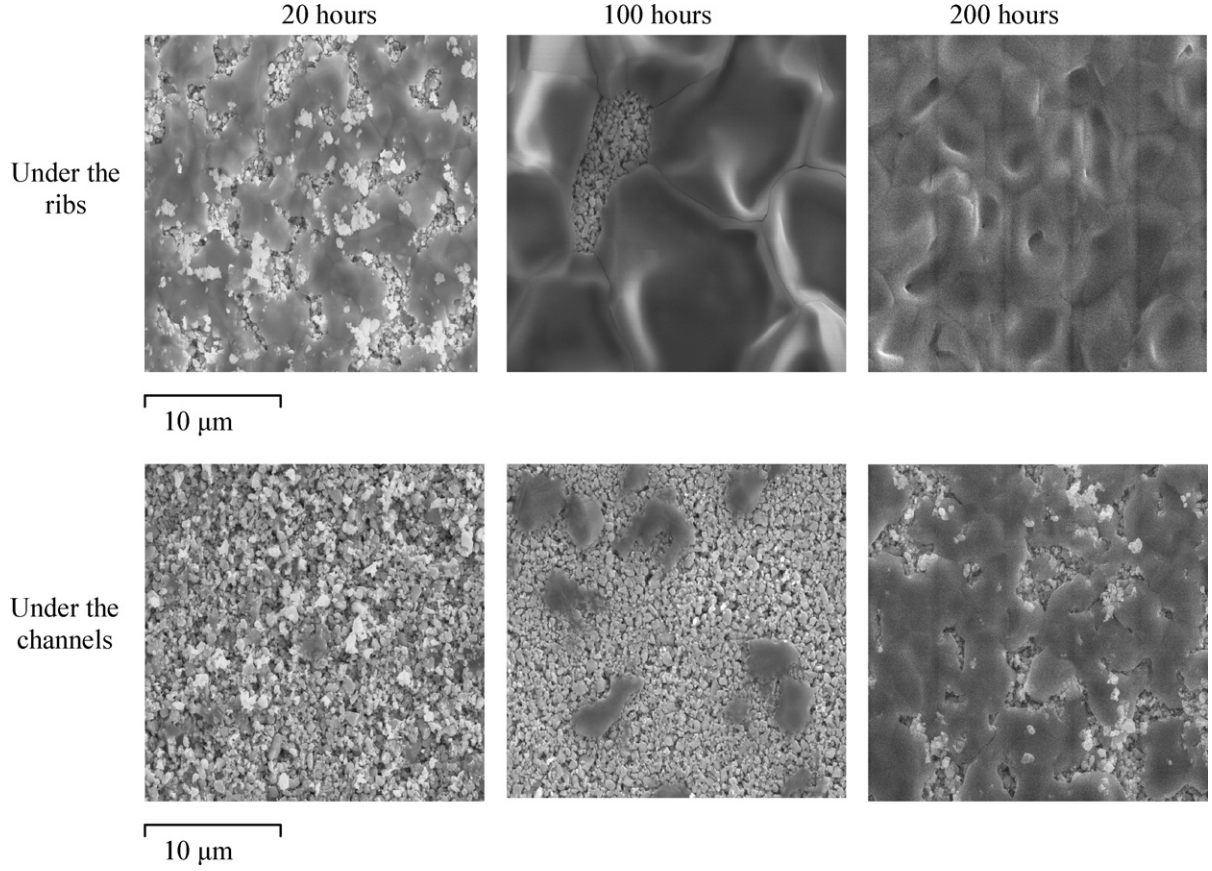

Fig. 4. Cathode surfaces after ageing at 700 °C in laboratory air.

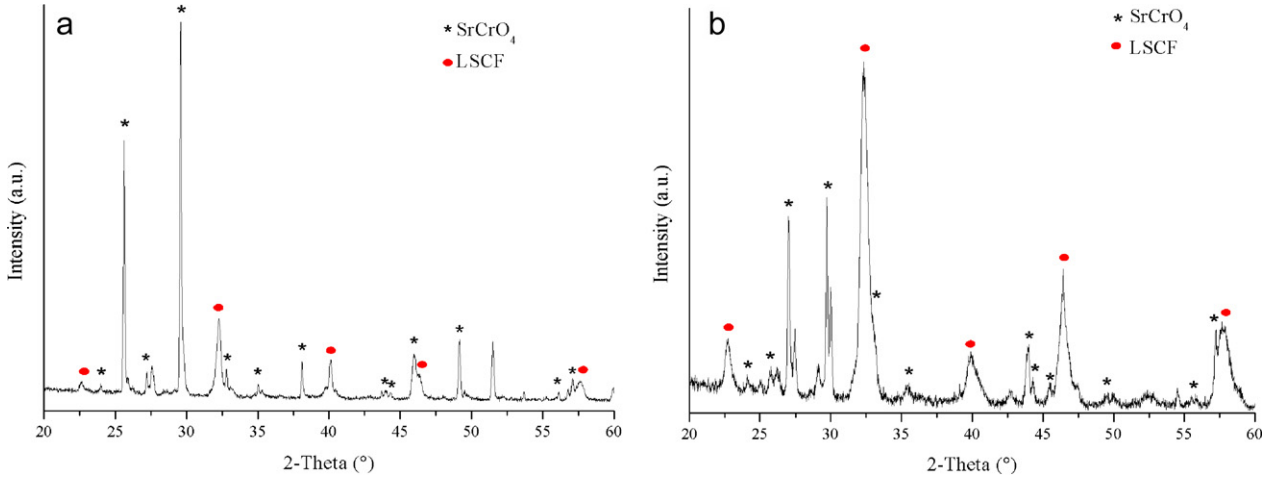

Fig. 5. Low angle XRD analysis of the surface of cathode sample (a) under the rib and (b) under the channel of the interconnect.

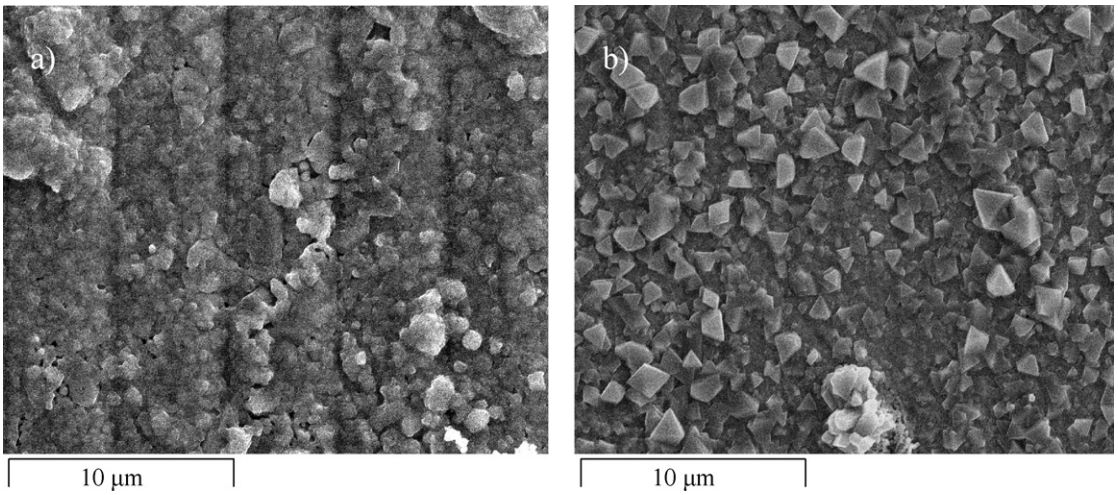

Fig. 6. Rib area on interconnect surface after ageing at 700 °C in laboratory air (a) in contact with cathode pellet, (b) not in contact with cathode pellet.

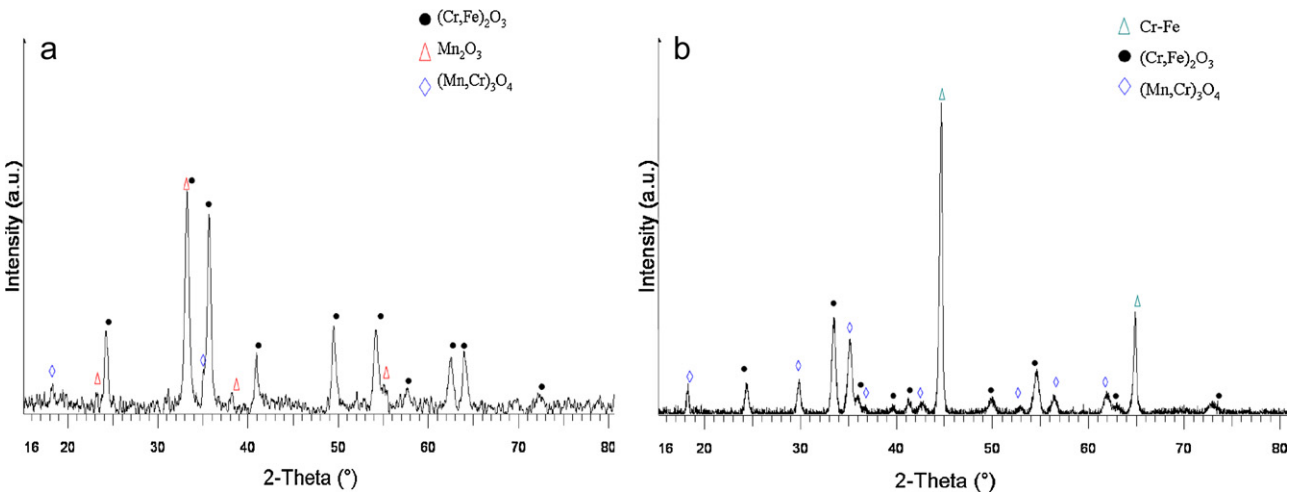

Fig. 7. Low angle XRD analysis of rib area on interconnect surface after ageing test at 700 °C, (a) in contact with cathode pellet, (b) not in contact with cathode pellet.

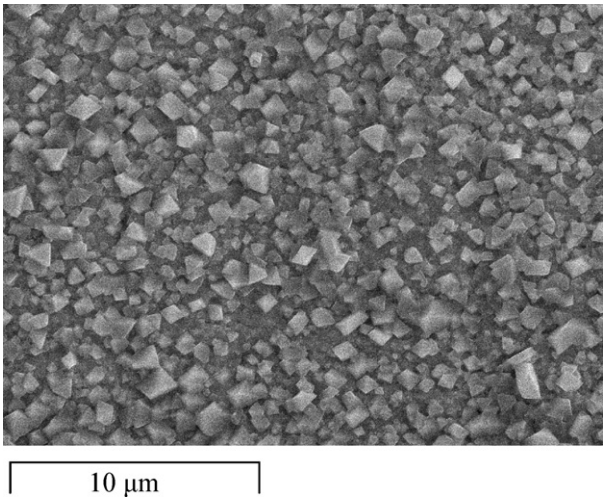

Fig. 8. Channel area on interconnect surface after ageing at 700 °C in laboratory air.

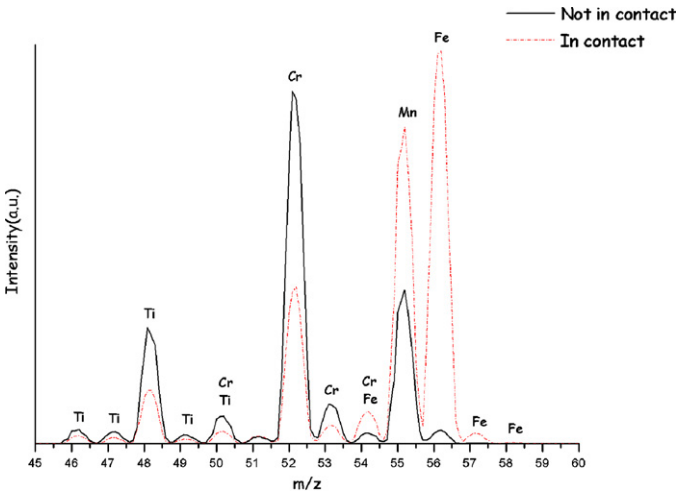

Fig. 9. SIMS analysis of interconnect surface after 200 h ageing at 700 °C in laboratory air with a LSCF cathode pellet.

3. Results

3.1. Ageing tests under air at 700 °C

Prior to ageing tests, LSCF cathode pellet was characterized. XPS analyses were achieved before and after sintering treatment (900 °C, 5 h). Even though original surface presented a deviation from expected stoichiometry, XPS analysis after sintering showed an enrichment of the surface in Sr and O (Table 2). We focused mainly on XPS spectra after sintering. Binding energy measurements were made with reference to the C 1s peak at 285 eV. The Sr $3d_{3/2}$ and $3d_{5/2}$ spectrum presents two doublets. The first is at binding energies 134.6 eV and 132.8 eV and the second at 136.0 eV and 134.5 eV (Fig. 3). Sr peaks are closed to the ones attributed to strontium surface and the occurence of two doublets indicate the presence of strontium in different chemical surrounding [31]. Moreover, Sr peak position at 132.8 eV and O 1s binding energy at 528.5 eV are consistent with SrO [32,33]. We noticed that an O 1s peak at 531.1 eV is observed. The attribution of this peak is not clear in literature and could arise from various sources: a carbonate, a hydroxyl group, a low coordinated oxygen ion [34–36]. During sintering treatment, Sr diffused through the bulk to the surface and combined with oxygen in order to form SrO.

Initially ageing tests were carried out under laboratory air. Reactivity study was first focused on cathode pellet. For both interfaces – under the rib and under the channel – dark big grains and smaller clearer grains are observed by SEM (Fig. 4). Under the ribs a coarsening of the dark big grains in function of ageing time can be observed. EDX analysis shows that small clear grains correspond to the cathode elements (La, Sr, Co and Fe). On the contrary, dark grains are formed by elements from the cathode and from the interconnect (Sr, Cr and O in molar ratio around 1:1:4). This new phase which appears at the cathode/interconnect interface during ageing tends to the $SrCrO_4$ composition. Low angle XRD patterns, presented in Fig. 5, confirm the formation of the $SrCrO_4$ phase at the different interfaces. Moreover, XPS analyses were carried out on cathode surface after treatments. Binding energy measurements were made with reference to the C 1s peak at 285 eV. The Sr 3d doublet position was determined near 133.6 and 135.8 eV. The O 1s peak position was found at 531.2 eV. Moreover, the Cr 2p bind-

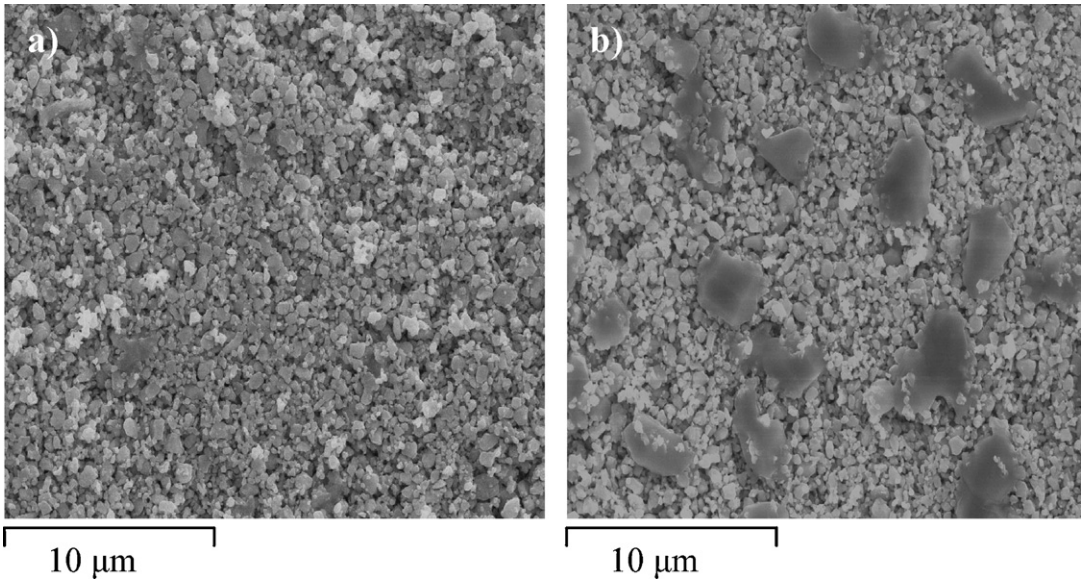

Fig. 10. Cathode surfaces (a) under the channel and (b) under the rib after ageing at 700 °C in dry air.

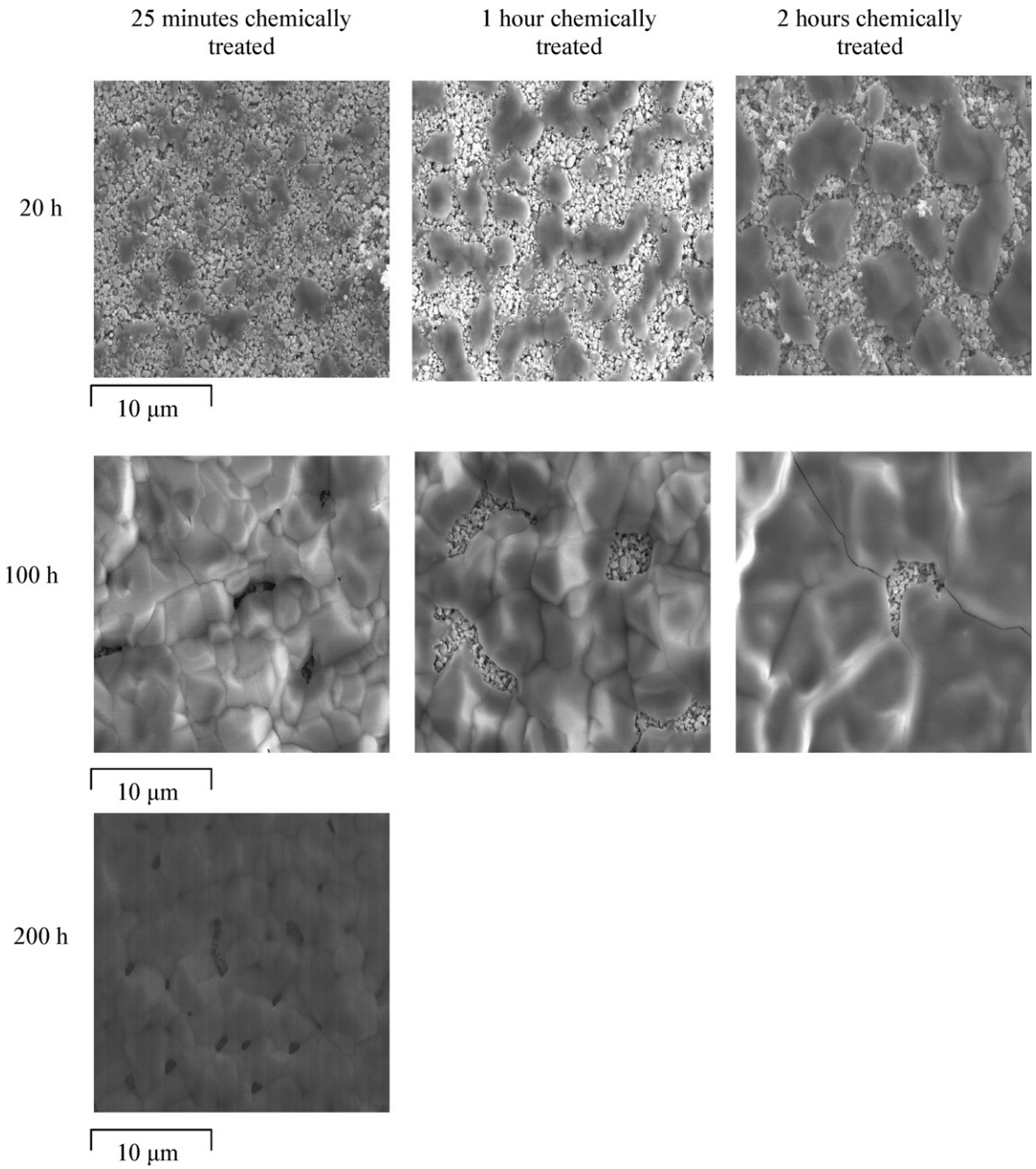

Fig. 11. Cathode surfaces under the ribs of interconnects after ageing at 700 °C in laboratory air.

ing energy was around 580.6 eV. These values, which are in good agreement with literature, are attributed to the $SrCrO_4$ compound [37,38].

Second, reactivity study was performed on interconnect. Morphology of surface rib area in contact with cathode pellet (Fig. 6(a)) is different from surface rib area not in contact (Fig. 6(b)). In this case cubic grains, which correspond to $(Cr,Mn)_3O_4$ spinel structure identified by low angle XRD (Fig. 7(b)), are observed for the top layer. Under this layer, chromia grains enriched in Fe are characterized. In the first case only one kind of grains seems to be present and cubic grains are not observed. XRD analysis (Fig. 7(a)) reveals the formation of Mn_2O_3, the presence of chromia enriched in Fe and $(Cr,Mn)_3O_4$, as minority phase. Morphology of surface channel area (Fig. 8) is similar to surface rib area not in contact with cathode pellet: $(Cr,Mn)_3O_4$ cubic grains as top layer and smaller chromia grains enriched in Fe as bottom layer can be observed. EDX analysis of channels and ribs reveals only the presence of Crofer22APU elements (Fe, Cr and Mn) and cathode characteristics elements (Co, La, Sr) are not detected.

SIMS analyses were carried out on interconnect surface aged 200 h at 700 °C in order to analyze the extreme surface diffusion (~2–3 nm). As shown in Fig. 9, only Crofer22APU typical elements (Fe, Cr, Mn and Ti) were detected in both interfaces (LSCF pellet in contact or not with the interconnect). So, there is no diffusion of La, Sr and Co from cathode to interconnect. The areas in contact with cathode pellet are richer in Fe and Mn, while the areas not directly in contact are richer in Cr. We can conclude that $(Cr,Mn)_3O_4$ spinel phase doesn't cover totally interconnect surface in the areas which have been directly in contact with cathode pellet, but a new phase (Mn_2O_3) formed.

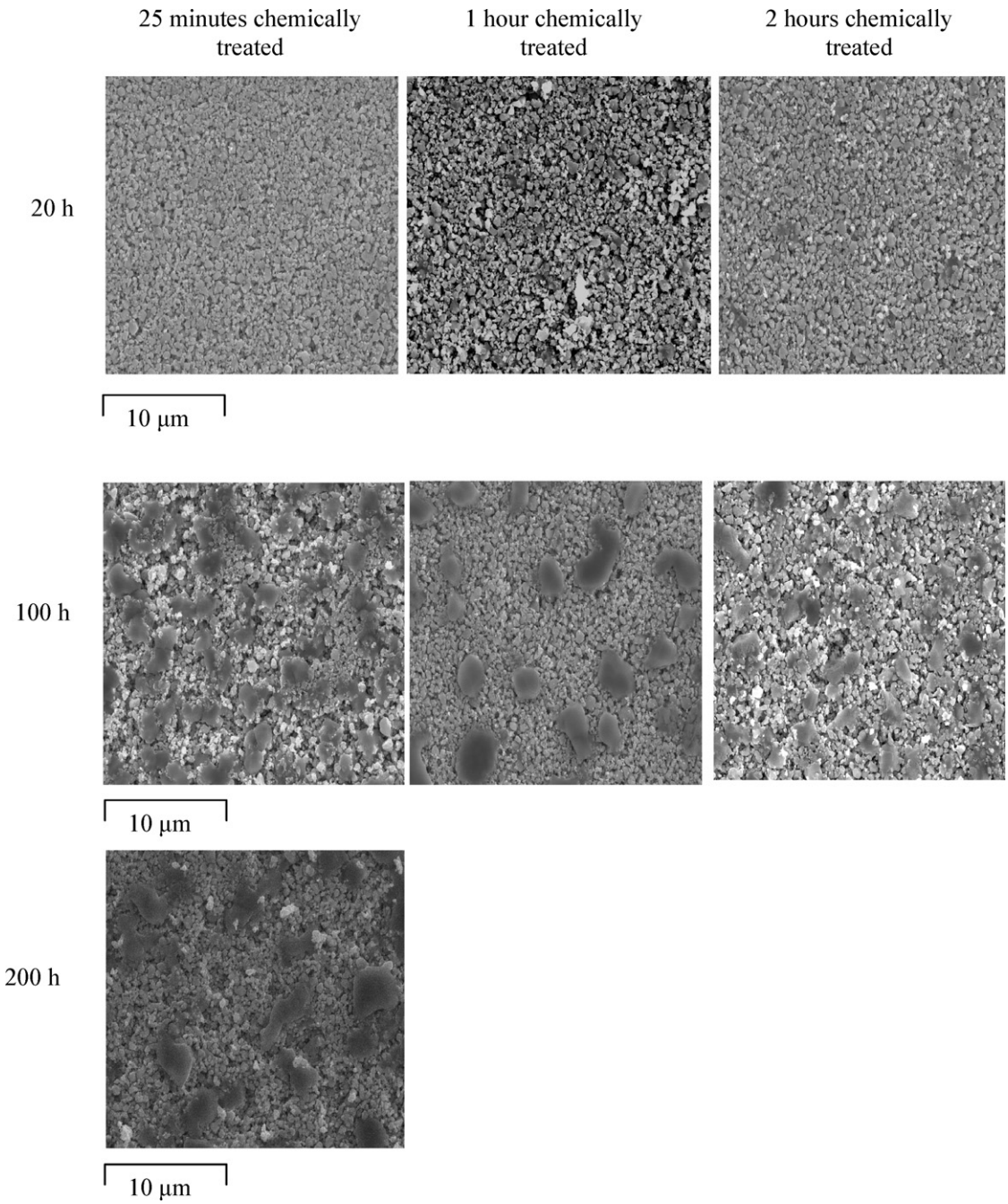

Fig. 12. Cathode surfaces under the channels of interconnects after ageing at 700 °C in laboratory air.

Additional ageing tests have been carried out for 100 h at 700 °C under dry air. SEM and EDX analyses performed on cathode pellet surfaces revealed that the growth of $SrCrO_4$ phase was avoided under channels and limited under ribs (Fig. 10).

3.2. Ageing tests in laboratory air after chemical etching

SEM micrographs of cathode surfaces under the ribs of interconnects are presented in Fig. 11. For all chemical etchings, two kinds of grains can be observed after 20 h of ageing. EDX analysis shows that dark grains are formed by Cr, Sr and O in molar ratio around 1:1:4. Based on the previous ageing tests, we affirm that it corresponds to $SrCrO_4$ grains. Between these grains, clearer smaller grains were formed by cathode elements. Note that an increase of the $SrCrO_4$ grain size is observed in function of chemical etching time (20 h ageing). For longer ageing test (100 h), the grains of the parasite phase formed a quite uniform layer on the cathode surface.

SEM micrographs of cathode surfaces under the channels of interconnects are presented in Fig. 12. Only one kind of grains can be observed after 20 h of ageing (cathode elements). On the contrary, $SrCrO_4$ isolated grains appeared for longer ageing test (100 and 200 h) and are separated by smaller grains formed by cathode elements.

Finally, interconnects surfaces were analyzed by SEM and EDX. Fig. 13 shows interconnect surface before chemical etching and oxidizing at 450 °C, but before ageing tests. Morphology presents roughness which are important to promote the adhesion of a cathode ink layer in the case of a contact layer is applied between the interconnect and electrode. After ageing tests at 700 °C, all surfaces observed have the same morphology. It is interesting to note that

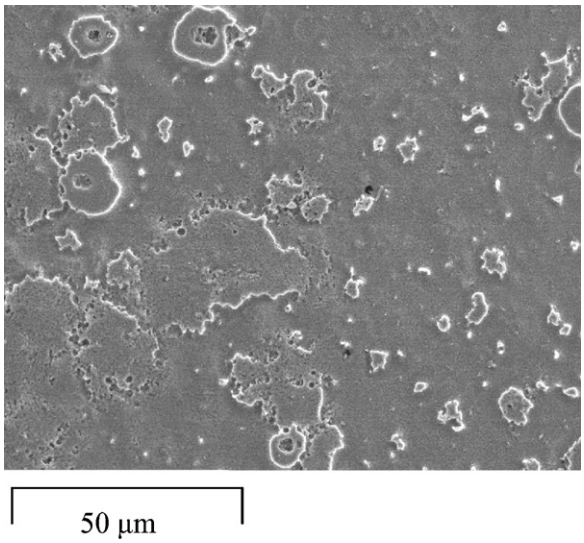

Fig. 13. Surface of interconnect after chemical etching and oxidizing at 450 °C.

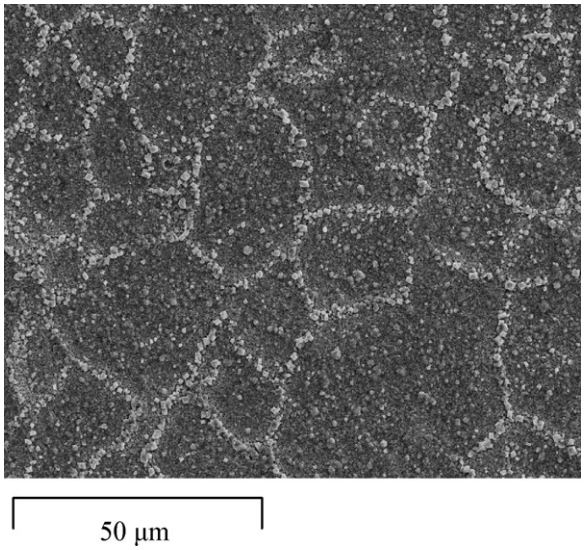

Fig. 14. Surface of the interconnect chemical etched after ageing at 700 °C in laboratory air.

cubic $(Cr,Mn)_3O_4$ spinel grains were more concentrated at grains boundaries (Fig. 14). This indicates that grain boundaries act as fast diffusion paths for Mn and Cr [39] in the case of the interconnects chemically etched.

4. Discussion

4.1. Mechanism proposed for $SrCrO_4$

Formation of parasite $SrCrO_4$ phase has been highlighted (SEM, XRD, XPS analyses), in the previous section, for both interfaces (rib and channel) after ageing and is in agreement with literature [6,21–23,40]. However, as presented on Fig. 4, the growth of this phase is depending on time and on interface type. On the surface of cathode sample, under the ribs of the interconnects, $SrCrO_4$ grains form a quite uniform layer in the case of 100 and 200 h ageing. On the contrary, the cathode surface under the channel of interconnect is not totally covered by the $SrCrO_4$ phase (for all ageing time) but an increase of the grain size in function of ageing time can be noticed (Fig. 4). This observation – changes in reaction rate in function of interface type – confirms that different physico-chemical mechanisms are involved.

We consider that transport of Cr from interconnect to cathode surface is probably dominated by solid phase diffusion under the rib. On the contrary, vapour phase diffusion of Cr species under the channel is suggested. These assumptions are in agreement with literature [6,22].

For solid state diffusion the follow mechanism is suggested:

$$SrO_{(s)} + (Cr, Mn)_3O_{4(s)} + O_{2(g)} \rightarrow SrCrO_{4(s)} + Mn_2O_{3(s)}$$

During solid state diffusion Cr from the $(Cr,Mn)_3O_4$ interconnect top layer reacts quickly with SrO formed at the cathode surface after sintering treatments and $SrCrO_4$ phase forms. Its formation, and the consequent chromium loss, destabilize $(Mn,Cr)_3O_4$ spinel phase which naturally formed on Crofer 22 APU surface during isotherm ageing. A new phase, Mn_2O_3, forms.

The vapour deposition process of Cr species on LSCF cathode surface, based on the one proposed by Jiang et al., can be written as follow [22,40]:

$$2Cr_2O_{3(s)} + 4H_2O_{(g)} + 3O_{2(g)} \rightarrow 4H_2CrO_{4(g)}$$

$$H_2CrO_{4(g)} + SrO_{(s)} \rightarrow SrCrO_{4(s)} + H_2O_{(g)}$$

The first step corresponds to the formation of chromia protective layer at the interconnect surface for high temperature. Then, water vapour present in laboratory air reacts with Cr evaporated from this layer in order to form chromium (VI) oxide or chromic (VI) acid. Chromium transport occurs primarily through the formation of Cr^{6+} containing species such as CrO_3 or H_2CrO_4 [41–43]. The partial pressure of CrO_3 is independent of moisture content. On the contrary, H_2CrO_4 partial pressure is directly depended on moisture content [44]. However, the dominant species in air containing moisture is H_2CrO_4. CrO_3 is also an important gaseous chromium species, but at low water contents and high temperatures (over 1000 °C) [45,46]. At this temperature its concentration in moist air is approximately as much as in dry air [46]. However CrO_3 is essentially not present at 700 or 800 °C [44,47].

So, in laboratory air and at 700 °C, Cr^{6+} species formed is chromic (VI) acid. The chromic gas compound combines with SrO formed at the cathode surface to produce $SrCrO_4$ parasite phase after sintering in the final step. The formation of the parasite phase is more significant at the rib interface, which indicates that the solid state diffusion is faster than gas phase reactions.

Results obtained under dry air confirm the gas phase mechanism suggested and the major role played by water vapour. Indeed gas phase reaction depends on the concentration of gaseous chromium compounds. They are greatly reduced working at 700 °C under dry air. It is interesting to note that formation of $SrCrO_4$ under ribs is resulting of two contributions: solid state reaction (always possible) and gas phase mechanism (greatly reduced under dry air).

To our point of view, under laboratory air, the contribution of gas reaction under the ribs is due to the surface roughness of the system. A small amount of gas can flow trough the interconnect/cathode solid interface and react with SrO (i.e. the solid interface is not completely gastight).

4.2. Chemical etching effects

An increase of $SrCrO_4$ grain size depending on chemical etching time can be noticed. This suggests that bigger grains – especially for 2 h chemical etching – were formed earlier to the other one (25 min and 1 h chemical etching). The 200 h ageing test shows that, even for the 25 min chemical etching, the $SrCrO_4$ layer covers much of cathode surface with a coarsening of the grains. Compared to the initial interconnect, the chemical etched Crofer22APU seems

to have a beneficial effect for the beginning period of ageing (20 h) for a chemical etching time equal at 25 min. Indeed, the formation of $SrCrO_4$ grains is reduced. But this treatment is not efficient to avoid the growth of $SrCrO_4$ layer under ribs for long term ageing (100 and 200 h).

Note that it is not necessary to extend chemical etching more than 25 min in order to obtain better protection. After ageing, cathode pellet surface in contact with Crofer22APU chemically etched is quite different from those without chemical etching. The formation of $SrCrO_4$ is avoided under 20 h ageing and decreased for 100 and 200 h. In fact, number and size of $SrCrO_4$ grains are reduced. Consequently, they were not in contact and cannot form a uniform parasite layer. The chemical etching permits to decrease the formation of $SrCrO_4$ layer under channels (even for 200 h ageing).

It seems that chemical etching promotes the growth of the spinel $(Cr,Mn)_3O_4$ phase at grain boundaries. Spinel phase did not act like a barrier for Cr solid state diffusion but it permitted to decrease the vaporization of Cr. This suggests that grain boundaries play a major role in the vapor phase reaction.

It will be interesting to perform a chemical etching shorter than 25 min. Moreover – in future works – development of protective coatings seems to be promising to avoid $SrCrO_4$ formation under ribs [19].

5. Conclusions

After ageing tests, formation of parasite $SrCrO_4$ phase was observed and characterized at the LSCF cathode/Crofer22APU interconnect interfaces. This phase growths very quickly at the cathode surface located under ribs of interconnects. On the contrary, $SrCrO_4$ phase formation is slower under channels of interconnects. In spite of different mechanisms involved under ribs and channels, Cr migration from Crofer22APU to LSCF is observed in both cases. Moreover, any cathode elements diffuse to the interconnect during ageing. Two mechanisms for $SrCrO_4$ formation were proposed: (i) fast solid state reaction under the ribs of interconnects, (ii) slower gas phase reaction under the channel of interconnects. Note that both mechanisms are depending on ageing time. Experiments carried out under dry air confirmed the suggested mechanism for gas phase reaction. Moreover, contribution of gas phase mechanism under the ribs was highlighted.

On interconnect rib in contact with cathode pellet XRD analysis showed the formation of a new phase (Mn_2O_3) after ageing. Cr migration during solid state diffusion causes Cr loss, $(Cr,Mn)_3O_4$ destabilization and subsequent Mn_2O_3 formation. This may become a problem for interconnect long term mechanical stability.

On one hand, the chemical etching performed on interconnects was not efficient to reduced $SrCrO_4$ formation under ribs for long ageing time. The spinel phase did not act like a barrier for Cr solid state diffusion. On the other hand, growth of parasite phase was decreased under channels after chemical etching. The promoted growth of the spinel phase at grain boundaries permitted to decrease the vaporization of Cr. This suggests that chemical etching is a method only to reduce locally, not to avoid completely, $SrCrO_4$ formation.

Acknowledgement

The research leading to these results has received funding from the European Community's Seventh Framework Programme (FP7/2007–2013) under grant agreement no 213389.

References

[1] Z. Zeng, K. Natesan, Solid State Ionics 167 (2004) 9.
[2] W.Z. Zhu, S.C. Deevi, Mater. Sci. Eng., A Struct. Mater. Prop. Microstuct. Process 348 (2003) 227.2.
[3] S.S. Hyung, G. Jin, J.H. Jun, D.H. Kim, K.Y. Kim, J. Power Sources 178 (2008) 1.
[4] C.J. Fu, K.N. Sun, N.Q. Zhang, X.B. Chen, D.R. Zhou, Thin Solid Films 516 (2008) 1857.
[5] C.L. Chu, J.Y. Wang, S.Y. Lee, Int. J. Hydrogen Energy 33 (2008) 2536.
[6] S.P. Jiang, J.P. Zhang, X.G. Zheng, J. Eur. Ceram. Soc. 22 (2002) 361.
[7] J.-H. Kim, R.-H. Song, S.-H. Hyun, Solid State Ionics 174 (2004) 185.
[8] J.W. Fergus, Mater. Sci. Eng. A 397 (2005) 271–283.
[9] W.J. Quadakkers, J. Piron-Abellan, V. Shemet, L. Singheiser, Mater. High Temp. 20 (2) (2003) 115.
[10] R. Hodja, W. Heimann, W.J. Quadakkers, Production-capable Materials Concept for High Temperature Fuel Cells, ThyssenKrupp Techforum, 2003, ISSN 1612–2771.
[11] P. Leone, M. Santarelli, P. Asinari, M. Calì, R. Borchiellini, J. Power Sources 177 (2008) 111.
[12] P. Plonczak, M. Gazda, B. Kusz, P. Jasinski, J. Power Sources 181 (2008) 1.
[13] P. Tsiakaras, G. Marnellos, C. Athanasiou, M. Stoukides, J.E. ten Elshof, H.J.M. Bouwmeester, H. Verweij, Solid State Ionics 86–88 (1996) 1451.
[14] W.-H. Kim, H.-S. Song, J. Moon, H.-W. Lee, Solid State Ionics 177 (2006) 3211.
[15] K. Świerczek, Solid State Ionics 179 (2008) 126.
[16] A. Thorel, A. Chesnaud, M. Viviani, A. Barbucci, S. Presto, P. Piccardo, Z. Ilhan, D. Vladikova, Z. Stoynov, ECS Trans. (SOFC XI) 25 (2) (2009) 753.
[17] A. Petric, P. Huang, F. Tietz, Solid State Ionics 135 (2000) 719.
[18] G. Caboche, J.-F. Hochepied, P. Piccardo, K. Przybylski, R. Ruckdäeschel, M.R. Ardigo, E. Fatome, S. Chevalier, A. Perron, L. Combemale, M. Palard, J. Prazuch, T. Brylewski, ECS Trans. (SOFC XI) 25 (2) (2009) 763.
[19] S. Fontana, R. Amendola, S. Chevalier, P. Piccardo, G. Caboche, M. Viviani, R. Molins, M. Sennour, J. Power Sources 171 (2007) 652.
[20] S. Chevalier, G. Bonnet, G. Brochardt, J.C. Colson, J.P. Larpin, Mater. Sci. Forum 369–372 (2001) 327.
[21] Y. Zhen, S.P. Jiang, J. Power Sources 180 (2008) 695.
[22] S.P. Jiang, Y. Zhen, Solid State Ionics 179 (2008) 1459.
[23] S.P. Jiang, S. Zhang, Y.D. Zhen, J. Electrochem. Soc. 153 (1) (2006) A127.
[24] K. Hilpert, D. Das, M. Miller, D.H. Peck, R. Weis, J. Electrochem. Soc. 143 (11) (1996) 3642.
[25] Z. Yang, G.G. Xia, G.D. Maupin, J.W. Stevenson, Surf. Coat. Technol. 201 (2006) 4476.
[26] H. Yokokawa, T. Horita, N. Sakai, K. Yamaji, M.E. Brito, Y.P. Xiong, H. Kishimoto, Solid state Ionics 177 (2006) 3193.
[27] J.Y. Kim, V.L. Sprenkle, N.L. Canfield, K.D. Meinhardt, L.A. Chick, J. Electrochem. Soc. 153 (5) (2006) A880.
[28] Z. Yang, G. Xia, P. Singh, J.W. Stevenson, J. Power Sources 155 (2006) 246.
[29] X. Montero, F. Tietz, D. Stöver, M. Cassir, I. Villarreal, J. Power Sources 188 (2009) 149.
[30] L. Bamoulid, PhD thesis, "Mise au point d'un nouveau photocatalyseur supporté sur un acier inoxydable pour la dépollution de l'eau", Université Paul Sabatier de Toulouse, Toulouse France (2007).
[31] R.H.E. van Doorn, H.J.M. Bouwmeester, A.J. Burggraaf, Solid State Ionics 111 (1998) 263.
[32] M.V. Bukhtiyarova, A.S. Ivanova, L.M. Plyasova, G.S. Litvak, V.A. Rogov, V.V. Kaichev, E.M. Slavinskaya, P.A. Kuznetsov, I.A. Polukhina, Appl. Catal. A: Gen. 357 (2009) 193.
[33] P.A.W. van der Heide, J. Electron. Spectrosc. Relat. Phenom. 151 (2006) 79.
[34] S. Kaliaguine, A. Van Neste, V. Szabo, J.E. Gallot, M. Bassir, R. Muzychuk, Appl. Catal. A: Gen. 209 (2001) 345.
[35] N.H. Batis, P. Delichere, H. Batis, Appl. Catal. A: Gen. 282 (2005) 173.
[36] M. Jiménez, A. Fernández, J.P. Espinós, A.R. González-Elipe, Spectrosc. Relat. Phenom. 71 (1995) 61.
[37] I.M. Baghni, S.B. Lyon, B. Ding, Surf. Coat. Technol. 185 (2004) 194.
[38] V. Murphy, S.A.M. Tofail, H. Hughes, P. McLoughlin, Chem. Eng. J. 148 (2009) 425.
[39] S. Chevalier, Traitements de surface et nouveau matériaux: quelles solutions pour lutter contre la corrosion à haute température? Editions Universitaires de Dijon collection Sciences, Dijon, 2007.
[40] X. Chen, L. Zhang, S.P. Jiang, J. Electrochem. Soc. 155 (11) (2008) B1093.
[41] E. Konycheva, U. Seeling, A. Besmehn, L. Singheiser, K. Hilpert, J. Mater. Sci. 42 (2007) 5778.
[42] C. Gindorf, K. Hilpert, L. Singheiser, Proc. Electrochem. Soc. (SOFC VII) 16 (2001) 793.
[43] B.B. Ebbinghaus, Combust. Flame 93 (1993) 119.
[44] J.W. Fergus, Int. J. Hydrogen Energy 32 (2007) 3664.
[45] M.C. Tucker, H. Kurokawa, C.P. Jacobson, L.C. De Jonghe, S.J. Visco, J. Power Sources 160 (2006) 130.
[46] E.J. Opila, Mater. Sci. Forum 461–466 (2004) 765.
[47] C. Gindorf, L. Singheiser, K. Hilpert, J. Phys. Chem. Solids 66 (2005) 384.